Fiber-ring laser intracavity QEPAS gas sensor using a 7.2 kHz quartz tuning fork

Qiang Wang [a], Zhen Wang [a], Wei Ren [a,*], Pietro Patimisco [b], Angelo Sampaolo [b], Vincenzo Spagnolo [b]

[a] Department of Mechanical and Automation Engineering, The Chinese University of Hong Kong, New Territories, Hong Kong
[b] PolySense Lab – Dipartimento Interateneo di Fisica, Politecnico di Bari and Università degli Studi di Bari, Via Amendola 173, Bari 70126, Italy

A B S T R A C T

A novel trace gas sensor exploiting fiber-ring laser intracavity quartz-enhanced photoacoustic spectroscopy (FLI-QEPAS) is reported. The gas sensor system couples an erbium-doped fiber-ring laser with a custom-designed quartz tuning fork (QTF) operating at 7.2 kHz. The QTF is placed in the fiber cavity to fully utilize intracavity optical power for photoacoustic excitation. We obtained a short intracavity absorption length of 1.5 cm, significantly extending the linear dynamic range of the gas sensor to an order of 10^5. As a proof of principle, the fiber laser was tuned to the C_2H_2 absorption line at 1531.6 nm. Operating at the optimal gas pressure and modulation depth selected for wavelength modulation spectroscopy, a minimum detectable C_2H_2 concentration of 29 ppbv at 300-s integration time has been achieved.

© 2018 Elsevier B.V. All rights reserved.

1. Introduction

Photoacoustic spectroscopy (PAS) is a trace gas detection technique that plays an important role in food safety, atmospheric chemistry and breath analysis applications [1–3]. It is a well-established spectroscopic technique with many advantages such as high sensitivity, high selectivity and fast time response [4,5]. In PAS, a sensitive microphone directly measures laser-absorption-induced acoustic waves without the need of photodetectors, which eliminates unwanted optical fringe interferences from windows, connectors and joints in the optical path [6–8] and allows for various types of laser sources from ultraviolet to terahertz.

Many recent researches focused on compact sensor design, cost effectiveness, and sensitivity enhancement by improving effective signals or/and suppressing optoelectronic noises. One attractive feature of PAS is that the photoacoustic signal is proportional to the incident laser power, so a higher laser power is always preferred in practical applications of PAS-based sensors. The laser power of a tunable seed laser can be boosted by a commercially available optical amplifier [9], which however has a capped ultimate power output. An alternative approach to build up the optical power is the employment of high-finesse optical cavity configurations, i.e., bow-tie [10], V-shaped [11] and Fabry-Perot [12]. However, an efficient

coupling of the laser beam into the external optical cavity requires a narrow laser linewidth and full overlap of laser frequency with the cavity transmission mode. All these conditions can be only achieved using sophisticated passive or active locking techniques. To fully exploit the laser power enhancement, the sensing element can be positioned directly inside the laser cavity, allowing an intracavity PAS detection [13–15]. We recently reported a novel fiber-ring laser intracavity PAS (or FLI-PAS) sensor by integrating a fiber-ring laser with a conventional PAS cell with a Q-factor of 4.9 [16].

Photoacoustic cell is a key element used in PAS for acoustic wave accumulation and amplification. Conventional PAS cells are sensitive to ambient background noises due to the wide response bandwidth of commercial microphones (several kHz). In comparison, a sharply resonant acoustic actuator with a response width below 1 Hz at low pressures, such as quartz tuning fork (QTF), can be used to replace microphones for photoacoustic detection. The QTF detection is immune to external sound sources, leading to the invention of quartz-enhanced photoacoustic spectroscopy (QEPAS) [17]. Commercial QTFs operating at a resonance frequency of ∼32 kHz have been widely implemented in QEPAS sensors because of their low cost and commercial availability [1–3,18–25]. However, collimated laser beams with spot sizes of 2–3 mm or larger must be properly focused through the 300 μm spacing gap of the 32 kHz-QTF prongs. Thus, a focusing lens combined with spatial filters is frequently used for beam shaping before directing the laser beam into the QEPAS gas cell. Recently, new types of QTFs with lower resonance frequencies (below 10 kHz) and larger prong spacing of
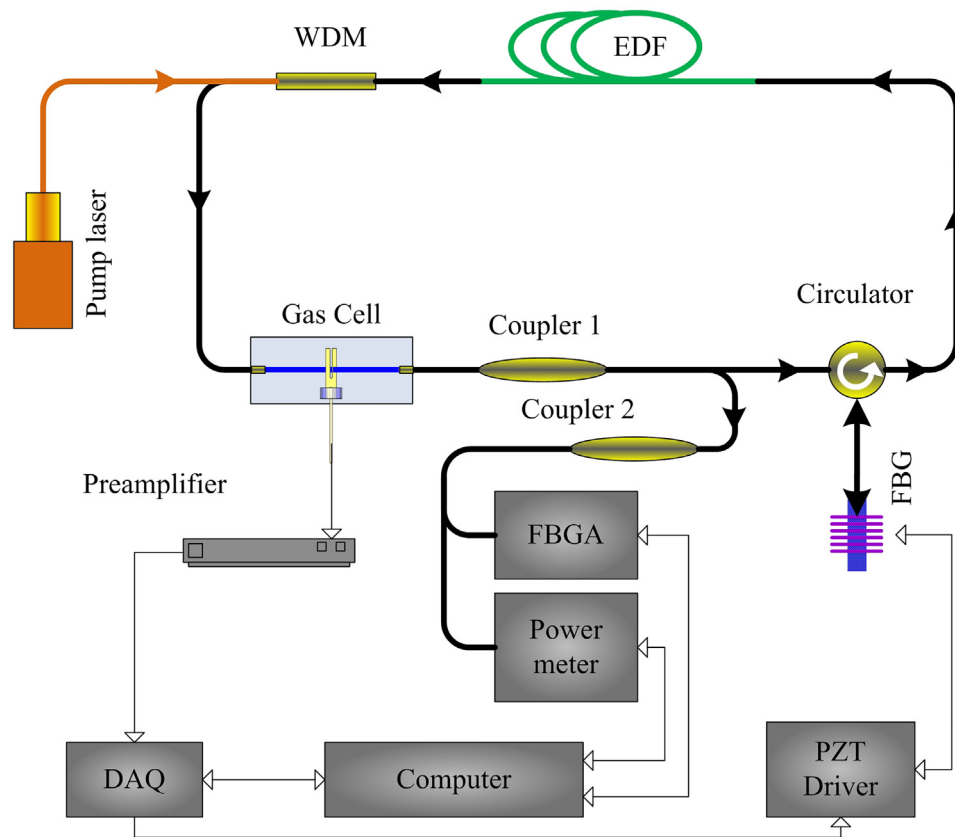
Fig 1. Schematic of the FLI-QEPAS C$_2$H$_2$ sensor. WDM, wavelength division multiplexer; EDF, erbium doped fiber; FBG, fiber Bragg grating; FBGA, FBG interrogation analyzer; PZT, piezoelectric transducer; DAQ, data acquisition card.

(∼1 mm) have been designed and realized [26,27]. These custom-designed QTFs have been successfully applied in QEPAS sensors using light sources with low-quality beam shapes such as fiber amplified lasers and THz lasers [9,26].

In this paper, a novel fiber-ring laser intracavity QEPAS (FLI-QEPAS) sensor for acetylene (C$_2$H$_2$) detection is reported. The sensor implements a custom-made QTF positioned inside a fiber-ring laser cavity. The QTF has a prong spacing of 800 μm, allowing a proper intracavity laser alignment using only one pair of C-lens single-mode fiber collimators. A continuous-wave fiber-ring tunable laser was developed using a fiber Bragg grating (FBG) to target the P(11) line of C$_2$H$_2$ at 1531.6 nm [28]. The small size of the employed QTF crystal allowed a short-path intracavity gas absorption length (1.5 cm), leading to a reduction of cavity losses induced by gas absorption, if compared with the previously developed FLI-PAS sensor [29]. The operating parameters of the developed sensor, such as gas pressure and modulation depth that can affect the detection sensitivity and linearity, have been systematically investigated.

2. Sensor configuration

Fig. 1 depicts the schematic of the FLI-QEPAS sensor for C$_2$H$_2$ detection. A fiber-ring laser with a spectral emission range 1520–1570 nm was realized using a single-mode erbium doped fiber (EDF) as the gain medium. The EDF was backwardly pumped by a 980-nm laser with a maximum emission power of 710 mW via a wavelength division multiplexer (WDM). A circulator was adopted to guarantee the backward propagation of laser light inside the fiber ring. The intracavity laser wavelength was selected by tuning a piezoelectric transducer (PZT) coupled with a FBG wavelength selector. A QEPAS sensing module employing the custom-made QTF

was placed in the laser cavity for photoacoustic detection. About 10% of the intracavity laser power was separated by coupler #1 for the purpose of optical power monitoring and wavelength calibration.

The compact QEPAS module shown in Fig. 2(a) (3 cm × 3 cm × 5 cm) was designed for FLI-QEPAS detection. A pair of C-lens single-mode fiber collimators were employed for intracavity laser coupling, reaching an efficiency of 80%. The collimated laser beam inside the cell has a diameter of 0.3 mm and thus can easily pass through the gap (0.8 mm) between the QTF prongs. The custom-made QTF was fabricated from a z-cut quartz wafer using photolithographic techniques, with chromium/gold contacts deposited on both sides of the QTF. The QTF used in this study has the same geometry of those employed in [9,27]; the prong length, width, and thickness are 10 mm, 0.9 mm, and 0.25 mm, respectively. It behaves like a standard 32-kHz QTF transducer but with a different Q factor and resonance frequency [27]. The QTF characterization is discussed in the next section.

The gas cell has a wall thickness of 6.5 mm to allow an easy mounting of the fiber collimators. The distance between the two C-lens collimators, corresponding to the effective gas absorption pathlength, is only 1.5 cm. Such a short absorption length mitigates the non-linear behavior of the intracavity gas sensor response induced by absorption losses occurring at higher gas concentrations [29]. The entire sampling volume was measured to be ∼10 mL. The vertical position of the collimated laser beam along the QTF axis between the prongs needs to be optimized in order to maximize the acoustic wave detection. When operating at the fundamental mode of the 7.2-kHz QTF, the optimal position of the laser beam was identified to be 1.2 mm below the free-end top of the prong, as shown by the red dot in Fig. 2(b) [30].
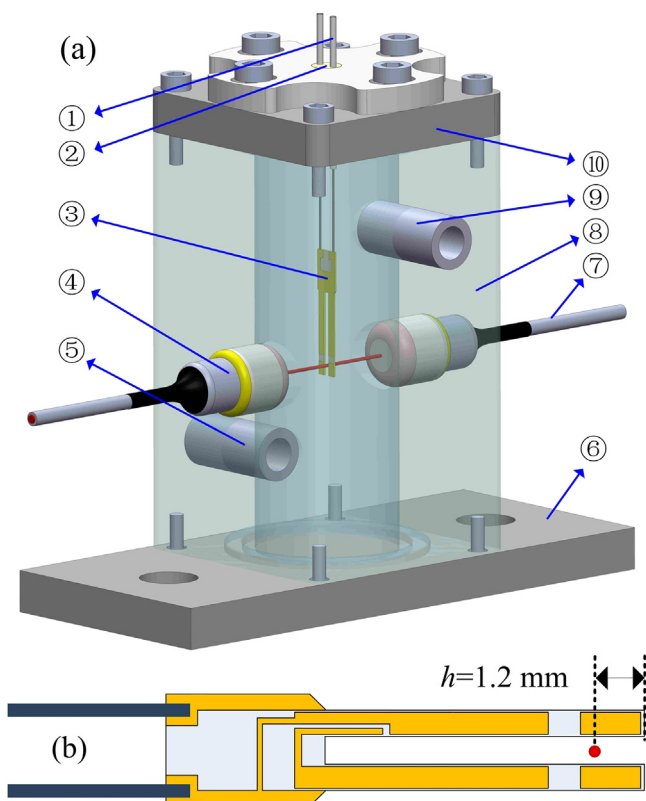
Fig. 2. (a) Schematic 3D view of the QEPAS sensing module implementing a custom-made QTF. 1, pins to be connected with the preamplifier; 2, QTF holder; 3, custom QTF operating at ~7.2 kHz; 4, C-lens collimator; 5, gas inlet; 6, bottom cover; 7, single mode fiber; 8, sealed gas cell; 9, gas outlet; 10, top cover. (b) In-plane view of the custom QTF with the laser beam positioned at $h = 1.2$ mm, as marked by the red dot. (For interpretation of the references to colour in this figure legend, the reader is referred to the web version of this article.)
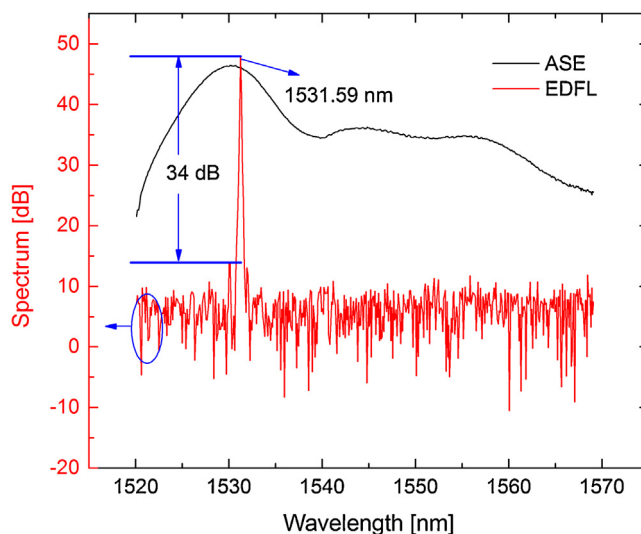

Fig. 3. Measured emission spectra of ASE (black solid line) and EDFL (red solid line). The y-axis refers to the EDFL spectrum. (For interpretation of the references to colour in this figure legend, the reader is referred to the web version of this article.)

Wavelength modulation and the second harmonic (2f) detection was used for QEPAS measurements, employing a FBG-based modulator. A digital signal generated by a data acquisition card (DAQ), controlled by a LabView-based software, was fed to a voltage amplifier, i.e. PZT driver (PiezoDrive, Au) driving the wavelength modulator. The QTF signal was amplified by a low-noise voltage amplifier (Sanford Research System, US) with a bandpass filter, which was further analyzed by a digital lock-in amplifier (LIA) to extract the 2f component.

3. Results and discussion

3.1. Tunable erbium doped fiber laser (EDFL)

Different from the previous study [29], a backward propagation configuration was implemented in this work to improve the pumping efficiency of the tunable EDFL. Fig. 3 depicts the amplified spontaneous emission (ASE) spectrum recorded by the FBGA. The ASE spectrum spans from 1520 nm to 1570 nm, wide enough to target the absorption features of several important molecules such as C_2H_2, CO, and H_2S [31]. As a proof of principle, we selected C_2H_2 for sensor demonstration, since it shows a strong absorption line-strength in this wavelength range. The selection of the fiber laser wavelength inside the ring cavity was achieved using a uniform FBG as wavelength selector. Fig. 3 shows a representative emission spectrum peaked at 1531.59 nm, proving a side-mode suppression ratio (SMSR) of 34 dB.

The intracavity laser power was extrapolated by using a 1:9 optical coupler [16] allowing to send ~10% laser power to the

power meter and FBGA system. The coupler #2 equally splits the optical power into two paths for simultaneous power monitoring and wavelength calibration. The results shown in Fig. 4(a) indicates a linear relationship between the intracavity laser power and the pump power. The threshold laser power was estimated to be 46 mW, and no saturation was observed at the highest available pump power level, proving an intracavity laser power of 460 mW. Higher intracavity laser power would require a stronger pump laser intensity.

The FBG was mounted on a high-speed PZT actuator to tune the EDFL wavelength by adjusting the PZT voltage [29]. Fig. 4(b) illustrates the tuning characteristics of EDFL wavelength and the corresponding optical power level, obtained by tuning the PZT voltage from 10 V to 100 V. The tuning range allows to scan across the P(11) line of C_2H_2 centered at 1531.59 nm. Within this PZT tuning range, the EDFL optical power remains approximately constant shown in Fig. 4(b).

WMS-2f detection is usually performed by dithering the laser current while slowly wavelength scanning across the selected absorption feature. We employed a different approach to achieve WMS in our sensor system. The EDFL wavelength was modulated by applying a 3.6-kHz sinusoidal waveform (10 V amplitude) to the PZT actuator, while tuned across the C_2H_2 absorption line by simultaneously feeding to the PZT a slow 100 mHz triangle waveform (56 V offset and 43 V amplitude). Fig. 5 depicts the measured laser power using the photodetector (InGaAs, Thorlabs, U.S.) along with the first half of the triangle waveform period. In the modulated EDFL scanning range, the laser power remains fixed at 23.5 mW, with a small standard deviation (1σ) of 0.016 mW. Hence, the modulated EDFL intracavity laser power is practically stable, with a noise level < -30 dB.

3.2. QTF characterization

The main electromechanical parameters of the QTF, namely the resonance frequency f_0 and the Q-factor, must be determined with high precision due to the ultra-narrow-band resonance mode profile. Both parameters are mainly determined by the quartz properties (Young modulus and density) and by the prong geometry [27], and also depending on the gas pressure. The resonance frequency and Q-factor of the QTF were measured by using a custom-designed control electronic unit, at different gas pressures
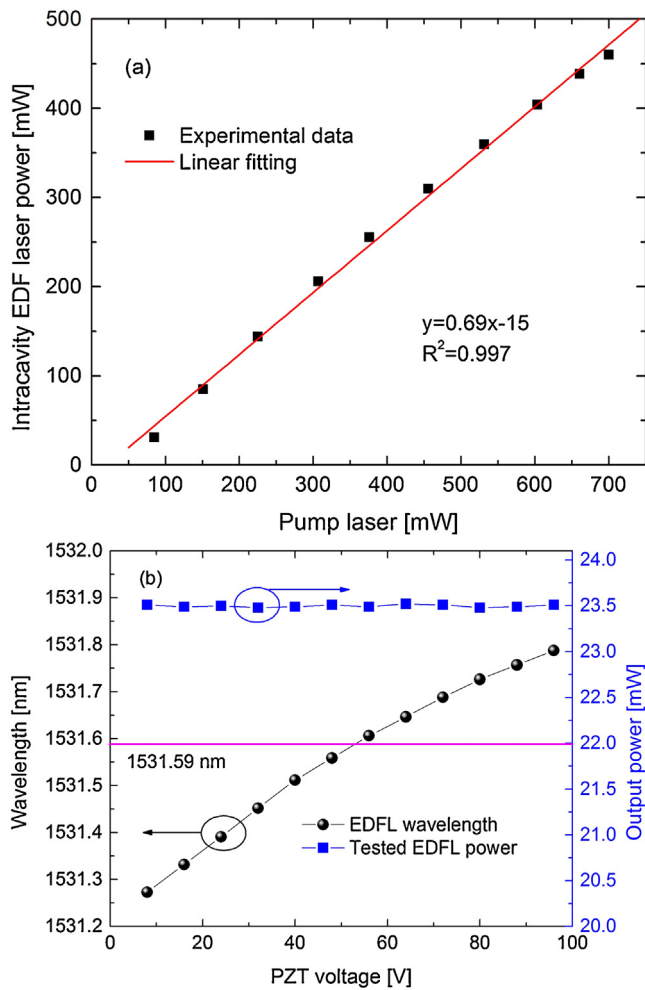
Fig. 4. EDFL calibration: (a) intracavity laser power as a function of pump laser power, and (b) tuning characteristics of laser wavelength and power.
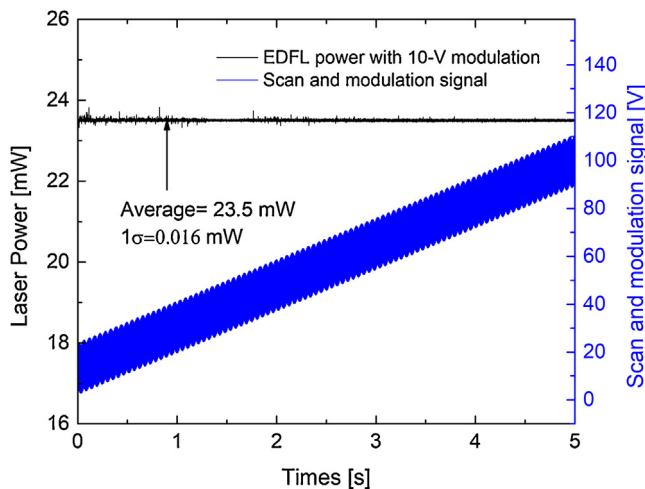

Fig. 5. EDFL power (black solid line) measured by the power meter with a modulated triangle waveform (blue solid lines) fed to the PZT actuator. (For interpretation of the references to colour in this figure legend, the reader is referred to the web version of this article.)
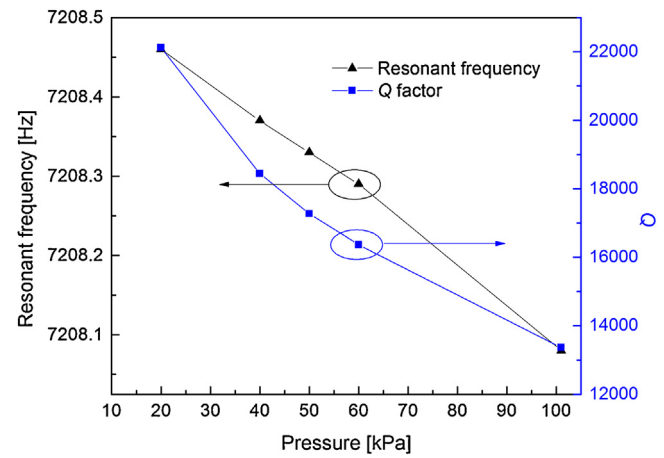

Fig. 6. Q-factor ($\blacksquare$) and resonance frequency ($\blacktriangle$) values measured for the QTF at different gas pressures.

using N_2 as the sample gas. Fig. 6 shows the QTF Q-factor and resonance frequency values, measured as a function of gas pressure. The QTF has a Q-factor of 22,100 at 20 kPa, and then decreases with gas pressures mainly because of the fluid damping influence [27,32]. Indeed, the fluid density increases with gas pressure, generating a corresponding increase of the QTF energy dissipation via the fluid damping effect in the vibrating prongs.

3.3. PZT modulation voltage and gas pressure selection

In QEPAS, the optimal wavelength modulation depth providing the highest QEPAS signal, in case of a Lorentzian absorption lineshape, corresponds to ~1.1 times the FWHM of the absorption profile [33]. In our experiment, this wavelength modulation depth value was obtained by properly modulating the PZT voltage. As the photoacoustic signal is directly proportional to the QTF Q factor, results are more beneficial to operate the QEPAS sensor at low gas pressures. However, molecular collisions at low gas pressures reduce the sound propagation efficiency [30]. Hence, a tradeoff gas pressure has to be experimentally determined in order to maximize the QEPAS signal. For this purpose, QEPAS signals measured for a gas mixture containing 900 part-per-million in volume (ppmv) of C_2H_2 in N_2 by changing the PZT modulation voltage from 3 to 10 V and the gas pressure in the range 20–101 kPa are shown in Fig. 7. Here, QEPAS signals were normalized to the highest obtained value. An almost identical trend is observed in the pressure range 40–60 kPa over the entire modulation voltage range. The sensor noise level remains unchanged in all the investigated pressures, as will be further discussed in Section 3.4. The optimal gas pressure and PZT modulation voltage values are found to be 60 kPa and 10 V, respectively.

3.4. Sensor linearity and stability

Using the optimal operating parameters for gas pressure and PZT modulation voltage, we investigated the linearity and stability of the FLI-QEPAS C_2H_2 sensor. A triangle signal (100 mHz, 54 V offset and 40 V amplitude) was used to slowly scan the laser wavelength across the selected C_2H_2 absorption line, while a sinusoidal dither ($f_0/2 = 3604.14$ Hz, 10 V amplitude) was used for wavelength modulation. The amplified signal was subsequently demodulated at the QTF resonance frequency f_0 with a detection bandwidth of 1 Hz. Different C_2H_2 concentrations in N_2 were generated using a commercial certified gas mixer (Jinwei Inc.). The lower acetylene concentrations (<1000 ppmv) were prepared starting from a
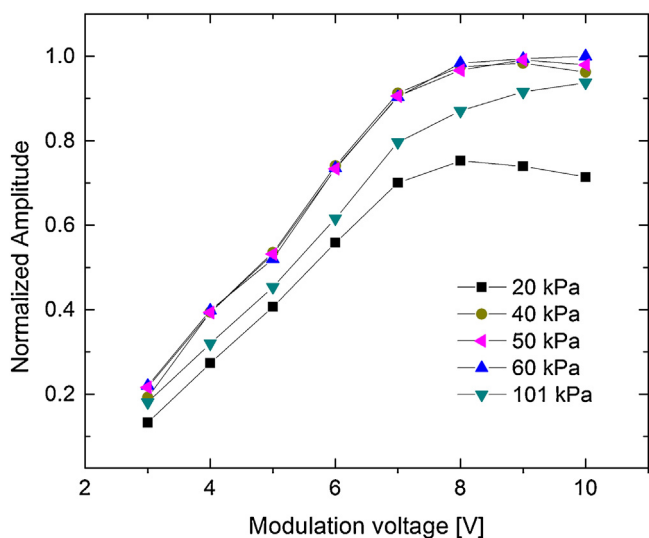
Fig. 7. Normalized QEPAS signals as a function of PZT modulation voltage for different gas pressures.
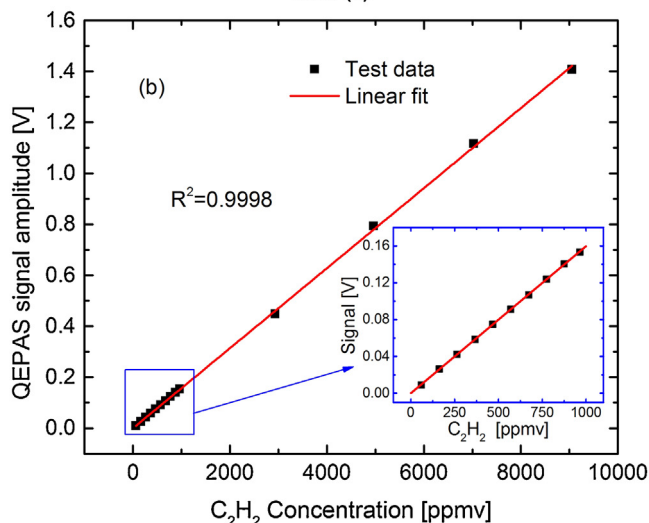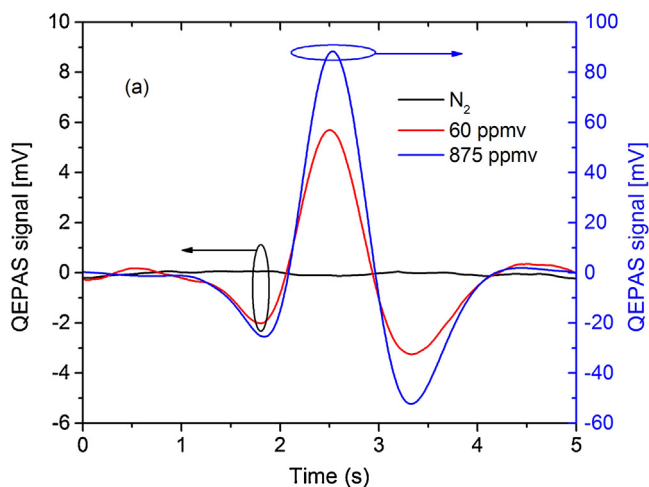

Fig. 8. (a) Representative QEPAS 2f signals measured at two different C_2H_2 concentrations; QEPAS signal acquired in pure N_2 is also shown. (b) QEPAS signal plotted as a function of C_2H_2 concentration. Inset: expanded view for the C_2H_2 concentrations <1000 ppmv.
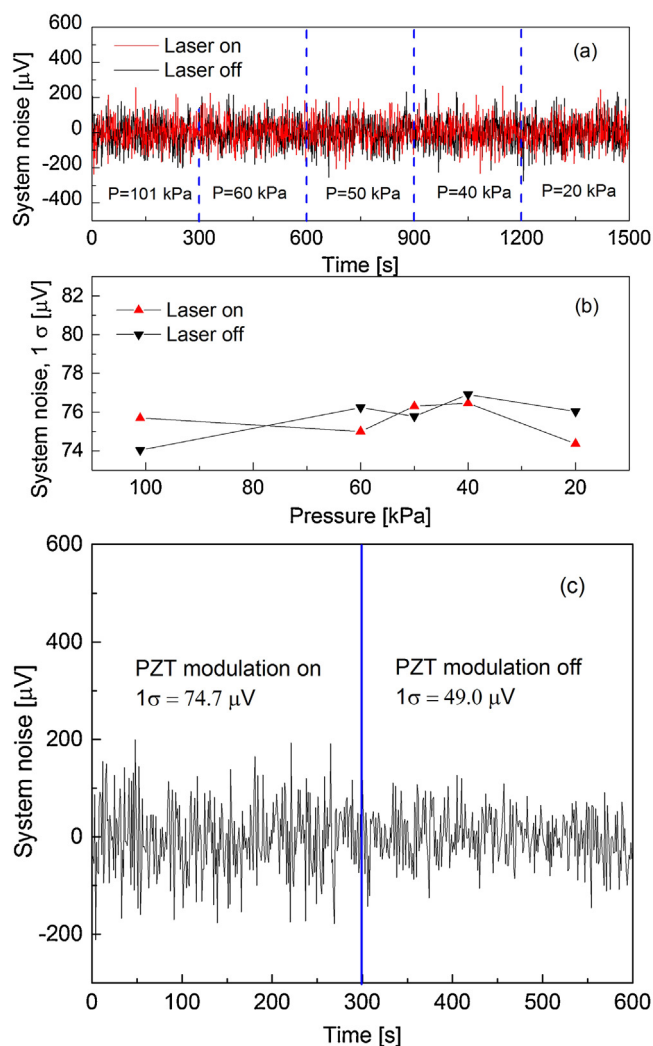

Fig. 9. (a) Comparison of system background noise at different gas pressures with the fiber laser on and off. (b) Measured system noise (1 σ) as a function of gas pressure with the fiber laser on and off. (c) Comparison of the sensor noise with fiber laser on while the PZT modulation is switched on and off.

certified 995 ppmv C_2H_2:N_2 gas mixture, whereas the higher concentration levels were generated employing a 1% C_2H_2:N_2 mixture.

Fig. 8(a) shows two representative QEPAS 2f-spectra obtained at two C_2H_2 concentrations, 60 ppmv and 875 ppmv; the signal measured for pure N_2 is also plotted. The asymmetry of the profile may be caused by the PZT hysteresis when performing wavelength modulation [34]. The sensor linearity was evaluated by measuring the QEPAS signals for a series of C_2H_2:N_2 mixtures at different concentrations. These measurements were performed in static state after pumping gas samples into the gas cell for about 2 mins. Fig. 8(b) plots the measured QEPAS signal amplitude (peak-to-peak) as a function of C_2H_2 concentration, ranging from 60 to 9100 ppmv. A linear fit to the experimental data yields an R-square value of 0.9998, indicating a good linear response with a slope of 6.4 ppmv/mV. Compared with our previous study using a conventional photoacoustic cell [29], the non-linearity behavior of the sensor response as a function of the C_2H_2 concentration was absent when using the current FLI-QEPAS configuration. This is mainly due to the reduced gas absorption length inside the laser cavity, resulting in the negligible influence of the absorption-induced cavity loss on the QEPAS signal. A wide linear dynamic range >10^5 was achieved by the demonstrated FLI-QEPAS C_2H_2 sensor.
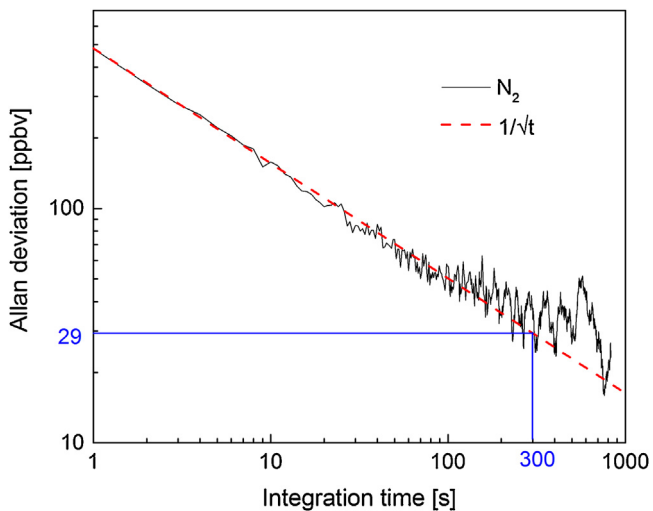
Fig. 10. Allan deviation analysis in ppbv for the FLI-QEPAS C_2H_2 sensor.

We also evaluated the dependence of sensor noise on gas pressure and intracavity laser power. The QEPAS signal for pure N_2 was recorded at different gas pressures from 20 kPa to 101 kPa by switching the fiber laser on and off. The acquired QEPAS signals are shown in Fig. 9(a). The standard deviation (1σ) values extracted from the QEPAS signals measured at different gas pressures are reported in Fig. 9(b). A similar 1σ noise level ($\sim 75\,\mu V$) was extracted for all the investigated pressures, indicating no contribution to the noise level by the laser radiation and the gas pressure. Note that the ultimate sensor noise level is determined by the thermal noise of the QTF, where the root mean square value (V_N) of its fluctuations is expressed as: $V_N = GR_F\sqrt{\frac{4KT}{R}\Delta f}$, where G is the gain of the low-noise voltage amplifier, R_F is the feedback resistor of the transimpedance preamplifier, K ($1.38 \cdot 10^{-23}\,m^2\,kg/s^2\,K$) is the Boltzmann constant, T (296 K) is the QTF temperature, R is the QTF electrical resistance and Δf is the lock-in detection bandwidth. Considering $G = 10$, $R_F = 10\,M\Omega$, $R = 346\,k\Omega$ and $\Delta f = 1\,Hz$ in this study, we estimated a thermal noise of $V_N = 22\,\mu V$. Hence, the other noise sources dominate the observed sensor noise level. Indeed, the QTF may be sensitive to the external noise at the resonance frequency of 7.2 kHz. Fig. 9(c) presents the influence of PZT modulation on system noise, showing a decrease of $\sim 35\%$ with the PZT modulation turned off.

To evaluate the long-term stability of the FLI-QEPAS sensor, an Allan deviation analysis was performed by measuring the QEPAS signal in pure N_2. A software-based wavelength stabilization scheme [35] was used to lock the laser wavelength to the C_2H_2 absorption peak by employing a 20 cm-long reference gas cell filled with 1% of C_2H_2:N_2. Fig. 10 reports the Allan deviation analysis showing that the ultimate detection limit scales as $1/\sqrt{t}$, where t is the lock-in integration time [36]. The calibration curve of the FLI-QEPAS sensor was used to convert the 1σ-noise voltages into C_2H_2 concentrations. A detection sensitivity of 29 part-per-billion in volume (ppbv) was achieved at 300 s, corresponding to a normalized noise equivalent absorption (NNEA) coefficient of $1.5 \times 10^{-8}\,cm^{-1}\,W\,Hz^{-1/2}$.

4. Conclusions

A novel gas sensor based on FLI-QEPAS technique was demonstrated for sensitive C_2H_2 detection, providing a large linear dynamic range in concentration. A backward pumped fiber-ring laser was used as an exciting photoacoustic source coupled with a custom QTF, realizing a detection module able to fully exploit the

intracavity laser power. A FBG-based modulator was designed to modulate the intracavity laser wavelength at half of the QTF resonant frequency (7.2 kHz), while maintaining the intracavity laser power constant over the entire wavelength scanning range. The FLI-QEPAS sensor achieved an ultimate detection sensitivity of 29 ppbv C_2H_2 in N_2 at a lock-in integration time of 300 s. Future work will be focused on implementing custom QTFs coupled with a single tube micro-resonator system to obtain a further enhancement in detection sensitivity [9,37–39].

References

[1] T. Nguyen Ba, M. Triki, G. Desbrosses, A. Vicet, Quartz-enhanced photoacoustic spectroscopy sensor for ethylene detection with a 3.32 μm distributed feedback laser diode, Rev. Sci. Instrum. 86 (2015) 023111.
[2] X. Yin, L. Dong, H. Wu, H. Zheng, W. Ma, L. Zhang, W. Yin, S. Jia, F.K. Tittel, Sub-ppb nitrogen dioxide detection with a large linear dynamic range by use of a differential photoacoustic cell and a 3.5 W blue multimode diode laser, Sens. Actuators B Chem. 247 (2017) 329–335.
[3] Z. Wang, Q. Wang, J.Y.L. Ching, J.C.Y. Wu, G. Zhang, W. Ren, A portable low-power QEPAS-based CO2 isotope sensor using a fiber-coupled interband cascade laser, Sens. Actuators B Chem. 246 (2017) 710–715.
[4] A. Miklós, P. Hess, Z. Bozóki, Application of acoustic resonators in photoacoustic trace gas analysis and metrology, Rev. Sci. Instrum. 72 (2001) 1937–1955.
[5] C. Haisch, Photoacoustic spectroscopy for analytical measurements, Meas. Sci. Technol. 23 (2011) 012001.
[6] J. Hodgkinson, R.P. Tatam, Optical gas sensing: a review, Meas. Sci. Technol. 24 (2012) 012004.
[7] P. Werle, Accuracy and precision of laser spectrometers for trace gas sensing in the presence of optical fringes and atmospheric turbulence, Appl. Phys. B 102 (2011) 313–329.
[8] G. Stewart, A. Mencaglia, W. Philp, W. Jin, Interferometric signals in fiber optic methane sensors with wavelength modulation of the DFB laser source, J. Lightwave Technol. 16 (1998) 43.
[9] H. Wu, A. Sampaolo, L. Dong, P. Patimisco, X. Liu, H. Zheng, X. Yin, W. Ma, L. Zhang, W. Yin, V. Spagnolo, Quartz enhanced photoacoustic H2S gas sensor based on a fiber-amplifier source and a custom tuning fork with large prong spacing, Appl. Phys. Lett. 107 (2015) 111104.
[10] S. Borri, P. Patimisco, I. Galli, D. Mazzotti, G. Giusfredi, N. Akikusa, M. Yamanishi, G. Scamarcio, P. De Natale, V. Spagnolo, Intracavity quartz-enhanced photoacoustic sensor, Appl. Phys. Lett. 104 (2014) 091114.
[11] A. Kachanov, S. Koulikov, F.K. Tittel, Cavity-enhanced optical feedback-assisted photo-acoustic spectroscopy with a 10.4 μm external cavity quantum cascade laser, Appl. Phys. B 110 (2013) 47–56.
[12] A. Rossi, R. Buffa, M. Scotoni, D. Bassi, S. Iannotta, A. Boschetti, Optical enhancement of diode laser-photoacoustic trace gas detection by means of external Fabry-Perot cavity, Appl. Phys. Lett. 87 (2005) 041110.
[13] F.J.M. Harren, F.G.C. Bijnen, J. Reuss, L.A.C.J. Voesenek, C.W.P.M. Blom, Sensitive intracavity photoacoustic measurements with a CO2 waveguide laser, Appl. Phys. B 50 (1990) 137–144.
[14] Z. Bozóki, J. Sneider, G. Szabó, A. Miklós, M. Serényi, G. Nagy, M. Fehér, Intracavity photoacoustic gas detection with an external cavity diode laser, Appl. Phys. B 63 (1996) 399–401.
[15] V.S. Starovoitov, J.F. Kischkat, M.P. Semtsiv, W.T. Masselink, Intracavity photoacoustic sensing of water vapor with a continuously tunable external-cavity quantum-cascade laser operating near 5.5 μm, Opt. Lett. 41 (2016) 4955–4958.
[16] Q. Wang, Z. Wang, J. Chang, W. Ren, Fiber-ring laser-based intracavity photoacoustic spectroscopy for trace gas sensing, Opt. Lett. 42 (2017) 2114–2117.
[17] A.A. Kosterev, Y.A. Bakhirkin, R.F. Curl, F.K. Tittel, Quartz-enhanced photoacoustic spectroscopy, Opt. Lett. 27 (2002) 1902–1904.
[18] P. Patimisco, G. Scamarcio, F.K. Tittel, V. Spagnolo, Quartz-enhanced photoacoustic spectroscopy: a review, Sensors 14 (2014) 6165–6206.
[19] K. Liu, X. Guo, H. Yi, W. Chen, W. Zhang, X. Gao, Off-beam quartz-enhanced photoacoustic spectroscopy, Opt. Lett. 34 (2009) 1594–1596.
[20] W. Ren, W. Jiang, N.P. Sanchez, P. Patimisco, V. Spagnolo, C.E. Zah, F. Xie, L.C. Hughes, R.J. Griffin, F.K. Tittel, Hydrogen peroxide detection with quartz-enhanced photoacoustic spectroscopy using a distributed-feedback quantum cascade laser, Appl. Phys. Lett. 104 (2014) 041117.
[21] H. Zheng, L. Dong, X. Yin, X. Liu, H. Wu, L. Zhang, W. Ma, W. Yin, S. Jia, Ppb-level QEPAS NO2 sensor by use of electrical modulation cancellation method with a high power blue LED, Sens. Actuators B Chem. 208 (2015) 173–179.

[22] Z. Wang, Z. Li, W. Ren, Quartz-enhanced photoacoustic detection of ethylene using a 10.5 μm quantum cascade laser, Opt. Express 24 (2016) 4143–4154.

[23] Z. Li, C. Shi, W. Ren, Mid-infrared multimode fiber-coupled quantum cascade laser for off-beam quartz-enhanced photoacoustic detection, Opt. Lett. 41 (2016) 4095–4098.

[24] Z. Li, Z. Wang, C. Wang, W. Ren, Optical fiber tip-based quartz-enhanced photoacoustic sensor for trace gas detection, Appl. Phys. B 122 (2016) 147.

[25] H. Yi, R. Maamary, X. Gao, M.W. Sigrist, E. Fertein, W. Chen, Short-lived species detection of nitrous acid by external-cavity quantum cascade laser based quartz-enhanced photoacoustic absorption spectroscopy, Appl. Phys. Lett. 106 (2015) 101109.

[26] S. Borri, P. Patimisco, A. Sampaolo, H.E. Beere, D.A. Ritchie, M.S. Vitiello, G. Scamarcio, V. Spagnolo, Terahertz quartz enhanced photo-acoustic sensor, Appl. Phys. Lett. 103 (2013) 021105.

[27] P. Patimisco, A. Sampaolo, L. Dong, M. Giglio, G. Scamarcio, F.K. Tittel, V. Spagnolo, Analysis of the electro-elastic properties of custom quartz tuning forks for optoacoustic gas sensing, Sens. Actuators B Chem. 227 (2016) 539–546.

[28] L.S. Rothman, I.E. Gordon, Y. Babikov, A. Barbe, D.C. Benner, P.F. Bernath, M. Birk, L. Bizzocchi, V. Boudon, L.R. Brown, A. Campargue, The HITRAN2012 molecular spectroscopic database, J. Quant. Spectrosc. Radiat. Transf. 130 (2013) 4–50.

[29] Q. Wang, Z. Wang, W. Ren, Theoretical and experimental investigation of fiber-ring laser intracavity photoacoustic spectroscopy (FLI-PAS) for acetylene detection, J. Lightwave Technol. 35 (2017) 4519–4525.

[30] F.K. Tittel, A. Sampaolo, P. Patimisco, L. Dong, A. Geras, T. Starecki, V. Spagnolo, Analysis of overtone flexural modes operation in quartz-enhanced photoacoustic spectroscopy, Opt. Express 24 (2016) A682–A692.

[31] A. Fomin, T. Zavlev, I. Rahinov, S. Cheskis, A fiber laser intracavity absorption spectroscopy (FLICAS) sensor for simultaneous measurement of CO and CO2 concentrations and temperature, Sens. Actuators B Chem. 210 (2015) 431–438.

[32] P. Patimisco, S. Borri, A. Sampaolo, H.E. Beere, D.A. Ritchie, M.S. Vitiello, G. Scamarcio, V. Spagnolo, A quartz enhanced photo-acoustic gas sensor based on a custom tuning fork and a terahertz quantum cascade laser, Analyst 139 (2014) 2079–2087.

[33] S. Schilt, L. Thévenaz, Wavelength modulation photoacoustic spectroscopy: theoretical description and experimental results, Infrared Phys. Technol. 48 (2006) 154–162.

[34] K. Liu, W.C. Jing, G.D. Peng, J.Z. Zhang, D.G. Jia, H.X. Zhang, Y.M. Zhang, Investigation of PZT driven tunable optical filter nonlinearity using FBG optical fiber sensing system, Opt. Commun. 281 (2008) 3286–3290.

[35] Q. Wang, Z. Wang, W. Ren, Wavelength-stabilization-based photoacoustic spectroscopy for methane detection, Meas. Sci. Technol. 28 (2017) 065102.

[36] M. Giglio, P. Patimisco, A. Sampaolo, G. Scamarcio, F.K. Tittel, V. Spagnolo, Allan deviation plot as a tool for quartz-enhanced photoacoustic sensors noise analysis, IEEE Trans. Ultrason. Ferroelectr. Freq. Control 63 (2016) 555–560.

[37] H. Zheng, L. Dong, A. Sampaolo, H. Wu, P. Patimisco, X. Yin, W. Ma, L. Zhang, W. Yin, V. Spagnolo, S. Jia, Single-tube on-beam quartz-enhanced photoacoustic spectroscopy, Opt. Lett. 41 (2016) 978–981.

[38] P. Patimisco, A. Sampaolo, L. Dong, F.K. Tittel, V. Spagnolo, Recent advances in quartz enhanced photoacoustic sensing, App. Phys. Rev. 5 (2018) 011106.

[39] H. Zheng, L. Dong, H. Wu, X. Yin, L. Xiao, S. Jia, R.F. Curl, F.K. Tittel, Application of acoustic micro-resonators in quartz-enhanced photoacoustic spectroscopy for trace gas analysis, Chem. Phys. Lett. 691 (2018) 462–472.

Biographies

Qiang Wang is currently a postdoctoral researcher at The Chinese University of Hong Kong. His current research interests focus on optical sensing and photoacoustic spectroscopy.

Zhen Wang is currently a Ph.D. student at The Chinese University of Hong Kong. His research project is on trace gas sensing and laser spectroscopy.

Wei Ren is currently an assistant professor in the Department of Mechanical and Automation Engineering at the Chinese University of Hong Kong. He received his B.S. degree in Mechanical Engineering and Automation in 2006 and M.S. degree in Optical Engineering in 2008 from the Department of Precision Instrument at Tsinghua University. He obtained his Ph.D. degree in Mechanical Engineering from Stanford University in 2013. After his graduate study, Dr. Ren worked as a Postdoctoral Fellow in the Department of Electrical and Computer Engineering at Rice University. Dr. Ren's research interests include laser spectroscopy, optical sensing, and combustion and propulsion.

Pietro Patimisco received the Master's (*cum laude*) and Ph.D. degrees from the University of Bari, Bari, Italy, in 2009 and 2013, respectively, both in physics. Since 2013, he has been a Postdoctoral Research Assistant with the University of Bari. He was a Visiting Scientist at the Laser Science Group, Rice University, Houston, TX, USA, from 2013 to 2014. His research interests include micro-probe optical characterization of semiconductor optoelectronic devices and optoacoustic gas sensors, the study and applications of trace-gas sensors, such as quartz enhanced photoacoustic spectroscopy and cavity-enhanced absorption spectroscopy in the mid-infrared and terahertz spectral region, leading to several publications, including a cover paper in the July 2013 issue of *Applied Physics Letters*.

Angelo Sampaolo received the Master's degree and Ph.D. degrees from the University of Bari, Bari, Italy, in 2013 and 2017, respectively, both in physics. Since April 2017, he is Research Assistant with the University of Bari. His research interests include the study of the thermal properties of heterostructured devices via Raman spectroscopy, development of innovative techniques in trace gas sensing based on quartz-enhanced photoacoustic spectroscopy and covering the full spectral range from near-IR to THz. His achieved results have been acknowledged by a cover paper in the July 2013 issue of *Applied Physics Letters*.

Vincenzo Spagnolo received the Ph.D. degree in physics from the University of Bari, Bari, Italy, in 1994. From 1997 to 1999, he worked as Researcher with the National Institute of the Physics of Matter (INFM). From 1999 to 2003, he was a Postdoctoral Research Associate with the Department of Physics, University of Bari. Since September 2015, he has been an Associate Professor with the Department of Physics, Polytechnic of Bari, Bari, Italy. His research activity is documented by more than 160 publications and 2 filed patents. He has given more than 40 invited presentations at international conferences and workshops. His research interests include quantum cascade lasers, spectroscopic techniques for real-time device monitoring, optoacoustic gas sensors. He has been visiting researcher at Rice University (Texas) in 2009 and 2010. He is the director of the joint-research Lab PolySense created by THORLABS GmbH and Technical University of Bari and devoted to the development and implementation of novel gas sensing techniques and the realization of highly sensitive QEPAS trace-gas sensors. Prof. Spagnolo is a Senior Member of the SPIE.